

1 Manuscript in Preparation

2

3 Range-wide differential adaptation and genomic vulnerability in
4 critically endangered Asian rosewoods

5

6 Tin Hang Hung^{1,*}, Thea So², Bansa Thammavong³, Voradol Chamchumroon⁴, Ida Theilade⁵,

7 Chhang Phourin², Somsanith Bouamanivong⁶, Ida Hartvig^{7,8}, Hannes Gaisberger^{9,10}, Riina

8 Jalonen¹¹, David H. Boshier¹, John J. MacKay^{1,*}

9 1. Department of Biology, University of Oxford, Oxford OX1 3RB, United Kingdom

10 2. Institute of Forest and Wildlife Research and Development, Phnom Penh, Cambodia

11 3. National Agriculture and Forestry Research Institute, Forestry Research Center,

12 Vientiane, Laos

13 4. The Forest Herbarium, Department of National Park, Wildlife and Plant

14 Conservation, Ministry of Natural Resources and Environment, Bangkok, Thailand

15 5. Department of Food and Resource Economics, Faculty of Science, University of

16 Copenhagen, Denmark

17 6. National Herbarium of Laos, Biotechnology and Ecology Institute, Ministry of

18 Science and Technology, Vientiane, Laos

19 7. Forest Genetics and Diversity, Department of Geosciences and Natural Resource

20 Management, University of Copenhagen, Denmark

21 8. Center for Evolutionary Hologenomics, Globe Institute, University of Copenhagen,

22 Denmark

23 9. Bioversity International, Rome, Italy

24 10. Paris Lodron University, Salzburg, Austria

25 11. Bioversity International, Serdang, Malaysia

26

27 Corresponding authors:

28 *T.H.H.: tin-hang.hung@biology.ox.ac.uk; *J.J.M.: john.mackay@biology.ox.ac.uk

29

30 **Classifications:** Biological sciences: Ecology

31 **Keywords:** rosewood, ecological genomics, climate vulnerability, adaptation

32

33 **Abstract**

34 In the billion-dollar global illegal wildlife trade, rosewoods have been the world's most
35 trafficked wild product since 2005¹. *Dalbergia cochinchinensis* and *D. oliveri* are the most
36 sought-after rosewoods in the Greater Mekong Subregion². They are exposed to significant
37 genetic risks and the lack of knowledge on their adaptability limits the effectiveness of
38 conservation efforts. Here we present genome assemblies and range-wide genomic scans of
39 adaptive variation, together with predictions of genomic vulnerability to climate change.
40 Adaptive genomic variation was differentially associated with temperature and precipitation-
41 related variables between the species, although their natural ranges overlap. The findings are
42 consistent with differences in pioneering ability and in drought tolerance³. We predict their
43 genomic offsets will increase over time and with increasing carbon emission pathway but at a
44 faster pace in *D. cochinchinensis* than in *D. oliveri*. These results and the distinct gene-
45 environment association in the eastern coastal edge suggest species-specific conservation
46 actions: germplasm representation across the range in *D. cochinchinensis* and focused on
47 vulnerability hotspots in *D. oliveri*. We translated our genomic models into a seed source
48 matching application, *seedeR*, to rapidly inform restoration efforts. Our ecological genomic
49 research uncovering contrasting selection forces acting in sympatric rosewoods is of
50 relevance to conserving tropical trees globally and combating risks from climate change.

51

52 **Significant statement**

53 In the billion-dollar global illegal wildlife trade, rosewoods have been the world's most
54 trafficked wild product since 2005, with *Dalbergia cochinchinensis* and *D. oliveri* being the
55 most sought-after and endangered species in Southeast Asia. Emerging efforts for their
56 restoration have lacked a suitable evidence base on adaptability and adaptive potential. We
57 integrated range-wide genomic data and climate models to detect the differential adaptation
58 between *D. cochinchinensis* and *D. oliveri* in relevance to temperature- and precipitation-
59 related variables and projected their vulnerability until 2100. We highlighted the stronger
60 local adaptation in the coastal edge of the species ranges suggesting conservation priority. We
61 developed genomic resources including chromosome-level genome assemblies and a web-
62 based application seedeR for genomic model-enabled assisted migration and restoration.

63 **Main**

64 Rosewoods have been the world's most trafficked wild product since 2005, amounting
65 to 30–40% of the global illegal wildlife trade¹, which is estimated at 7–23 billion USD
66 annually⁴. *Dalbergia cochinchinensis* Pierre and *D. oliveri* Gamble ex Prain are among the
67 most sought-after and threatened rosewood species. Exploited for their extremely valuable
68 timber², alongside many other valued and threatened tree species in Asia's tropical and
69 subtropical forests⁵, the growing demand and limited supply have driven prices as high as
70 50,000 USD per cubic metre⁶. Both these *Dalbergia* species were classified as Vulnerable
71 and Endangered in the 1998 IUCN Red List^{7,8}. The Convention on International Trade in
72 Endangered Species of Wild Fauna and Flora (CITES) has listed the entire *Dalbergia* genus
73 in its Appendix II since 2017 to reduce sequential exploitation of other closely related
74 species⁹. In the IUCN's latest re-assessment of their endangered status to Critically
75 Endangered in 2022^{10,11}, it is suspected that the populations of both species have already
76 experienced a decline of at least 80% over the last three generations, and the decline is likely
77 to continue¹².

78 *D. cochinchinensis* and *D. oliveri* are sympatric species, endemic to the Greater Mekong
79 Subregion (GMS) in Southeast Asia, an area of high ecological and conservation concern as
80 84% of the GMS overlaps with the Indo-Burmese mega biodiversity hotspot¹³. The complex
81 biogeographical and geological histories of the GMS have contributed to its high species
82 richness, heterogeneous landscapes, and high endemism levels¹⁴. Ancient changes in the
83 distribution of terrestrial and water bodies have been associated with changes in vegetation
84 types and cover¹⁵. These forests contribute substantially to local livelihoods, economies, food
85 security, and human health^{16,17}, though overexploitation undermines their potentially central
86 role to nature-based solutions and most of them are unprotected⁴.

87 Species- and environment- specific conservation approaches represent an immediate
88 need in response to declining populations⁵. Conservation, collection, and use of genetically
89 diverse germplasm are key to conserving diversity and restoring these rosewood populations.
90 Genetic conservation actions were started in the early 2000s but were limited in scale, usually
91 including fewer than 50 seed-producing trees per country^{18–20}. Newer capacity-building
92 initiatives targeting tree nurseries and seed value chain development²¹ may still carry genetic
93 risks associated with the supply and use of germplasm, and may compound the effects of
94 over-exploitation. First, underrepresented genetic diversity during the sourcing of genetic
95 materials can create a genetic bottleneck for the species and reduce the species' ability to
96 adapt and evolve in a changing climate²². Second, mismatch of habitat suitability can result in
97 maladaptation, if populations have strong local adaptation²³. Third, climate change will likely
98 impose new forces of selection on the current genetic diversity, thus reducing the species'
99 adaptability, affecting population functioning^{24,25}, and leading to increased risk of local
100 extirpations and species' range collapse²⁶. If unaddressed, these risks will reduce both short
101 and long-term effectiveness of restoration projects. The genetic risks call for an
102 understanding of adaptation and its genetic basis in *Dalbergia* species in the GMS to
103 safeguard on-going conservation and restoration efforts. *Dalbergia* are high value species that
104 could be used sustainably and generate income for farmers in developing countries if well-
105 adapted planting material is available⁵. Planting for economic purposes and reducing risks to
106 remaining natural populations of these species seem necessary, where ecological restoration
107 alone is insufficient.

108 Of the 14,191 vascular plants that are listed as either Vulnerable, Endangered, and
109 Critically Endangered in the IUCN Red List, only 0.1% have their genomes published, far
110 fewer than the 1% reported for listed animals²⁷. There is a critical lack of genomic resources
111 in threatened species and a disproportionate representation across taxa, in contrast with the

112 rapid growth in genomic technologies. New reference genomes in threatened species will
113 enable the analysis, of functional genes, higher-resolution studies of species delineation,
114 association mapping and adaptation, genetic rescue, and genome editing²⁸. These in turn will
115 help to address important conservation (and restoration) questions such as genetic monitoring
116 of introduced and relocated populations, predicting population viability, disease resistance,
117 synthetic alternatives, and de-extinction^{29,30}.

118 This paper develops an unprecedented understanding of adaptation in critically
119 endangered rosewoods, which integrates genomic analyses, the creation of a novel evidence,
120 and a resource base to inform and expand ongoing conservation efforts. (1) We present
121 genome assemblies of *D. cochinchinensis* and *D. oliveri* at chromosomal and near-
122 chromosomal scale respectively. (2) We analyse range-wide patterns of adaptation by
123 genotyping ~800 trees, and identify differential drivers of adaptive genetic diversity between
124 the two species by using gene-by-environment association analyses. (3) We project current
125 genotypes onto future climate scenarios and predict the potential maladaptation of
126 populations. (4) We deploy an interactive application to predict optimal seed sources, based
127 on our landscape genomic results, in *D. cochinchinensis* and *D. oliveri* for use in restoration
128 under future climate scenarios. Our ecological genomic study in the GMS fills crucial
129 knowledge gaps for genomic adaptation in tropical tree species which are highly
130 underrepresented in the current research literature.

131

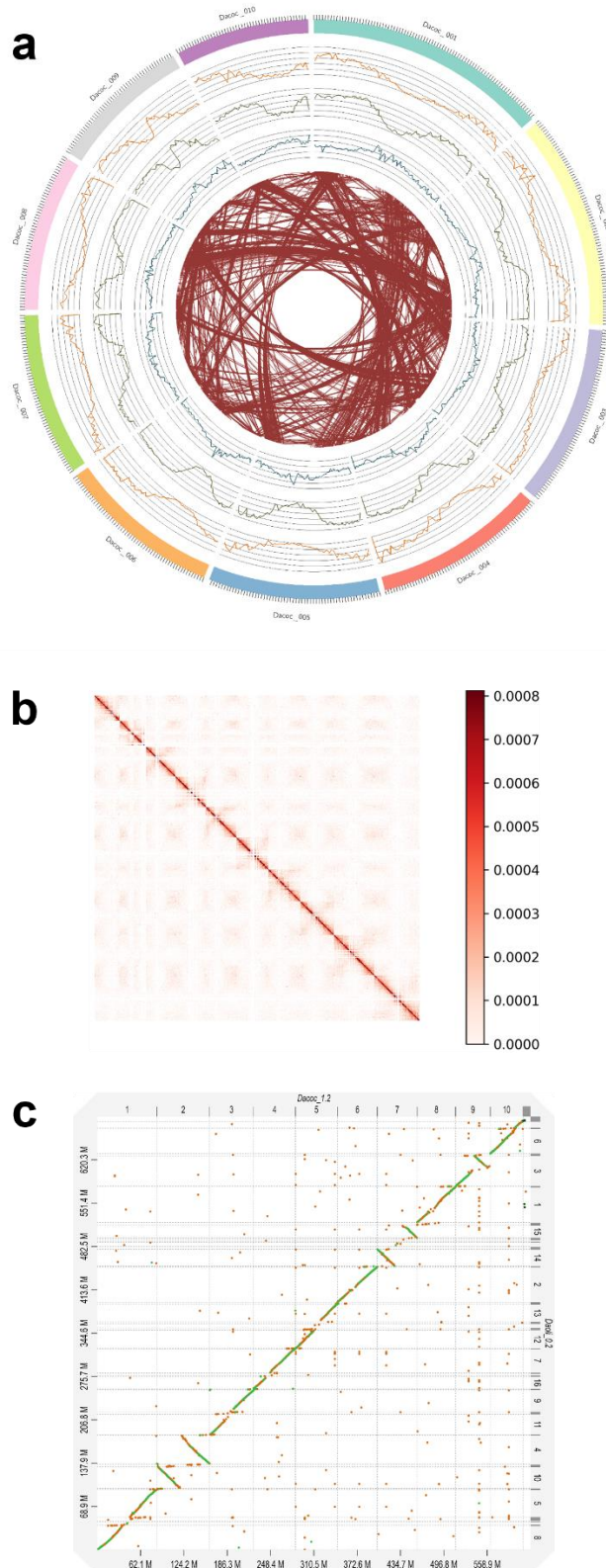
132 **Chromosome-scale genome characterisation**

133 The *D. cochinchinensis* reference genome assembly (Dacoc_1.4) was 621 Mbp in size
134 comprised of 10 pseudochromosomes (Figure 1a, Supplementary Figure 1, Supplementary
135 Table 1). Whole-genome sequencing of a single seedling of *D. cochinchinensis* produced 165
136 Gbp (~260 X) long-read data. A diploid-aware draft assembly of 1.3 Gbp with 6,443 contigs

137 and a N50 of 1.35 Mbp was first obtained, with the longest contig between 33.2 Mb at
138 chromosome-arm length. We purged the haplotig and scaffolded the draft genome with 54.97
139 Gbp (~88.52X) Hi-C chromosome conformation capture reads into 511 scaffolds with a N50
140 of 60.0 Mb (Supplementary Table 2). The 10 longest scaffolds were considered
141 pseudochromosomes and 98.3% of the contigs were mapped onto them (Figure 1b).

142 The *D. oliveri* draft genome assembly (Daoli_0.3) was 689.25 Mbp in size
143 (Supplementary Figure 1, Supplementary Table 3). Whole-genome sequencing of a single
144 seedling of *D. oliveri* produced 15.13 Gbp (~22X) long-read data. We first obtained a
145 diploid-aware draft assembly of 814.69 Mbp with 3,249 contigs and a N50 of 474.02 Kbp.
146 We purged the haplotig and scaffolded the draft genome with 13.46 Gbp (~20X) Pore-C
147 multi-contact chromosome confirmation capture reads into 2,977 scaffolds with a N50 of
148 38.43 Mbp. Syntenic analysis of the *D. oliveri* assembly (Daoli_0.3) against the 10
149 pseudochromosomes obtained in *D. cochinchinensis* (Dacoc_1.4) showed that the 16 largest
150 scaffolds in Daoli_0.3 had 1-to-1 or 2-to-1 correspondences to Dacoc_1.4, implying that
151 Daoli_0.3 was at chromosome-arm length (Figure 1c).

152 We constructed *de novo* repeat libraries of Dacoc_1.4 and Daoli_0.3, which contained
153 402 Mbp and 453 Mbp of repeat elements respectively (64.80% and 65.71% of the genomes)
154 (Supplementary Table 4, Supplementary Table 5), the majority of which were annotated as
155 containing LTR elements (46.63% and 48.55%) such as Ty1/Copia (15.25% and 15.75%) and
156 Gypsy/DIRS1 (30.51% and 31.96%). The repeat content of the two genomes was
157 significantly higher than the average among Fabids (~49%), which may be due to the near
158 double amount of LTRs (~22%)³¹.



159

160 **Figure 1.** (a) Genomic landscape of the 10 assembled pseudochromosomes of *D. cochinchinensis* (Dacoc_1.4), showing tick
161 marks every 1 Mb, gene density (orange), repeat density (green), 5-mC density (blue), and interchromosomal syntenic
162 arrangement (brown). The densities are calculated in 1-Mb sliding window. (b) High-resolution contact probability map of
163 the final *D. cochinchinensis* genome assembly after scaffolding, revealing the 10 pseudochromosomes at 100 Kbp resolution.
164 (c) Syntenic dot plot of assemblies of *D. oliveri* (Daoli_0.3) against *D. cochinchinensis* with a minimum identity of 0.25.

165 We predicted and annotated 27,852 and 33,558 gene models in Dacoc_1.4 and
166 Daoli_0.3 respectively, using previous RNA sequencing data (Supplementary Table 6) and
167 protein homology of *Arabidopsis thaliana* and *Arachis ipaensis*. The gene models had a mean
168 length of 4,284.20 and 3942.71 bp respectively, of which 98.3% and 95.5% had an AED
169 score less than 0.5, considered as strong confidence (Supplementary Figure 2). The gene
170 models had a BUSCO v5.1.2 completeness of 96.2% and 88.3% using the eudicots_odb10
171 reference dataset, with 92.1% and 86.7% being both complete and single copy.

172

173 **Range-wide genomic scan for adaptive signals**

174 We obtained initial pools of 1,832,629 and 3,377,855 SNPs from genotyping 435 and
175 331 individuals of *D. cochinchinensis* and *D. oliveri* respectively, across their natural ranges
176 (Supplementary Table 7), and final pools of 180,944 and 193,724 SNPs after filtering for
177 missing data, minimum allele frequency, and linkage disequilibrium. The samples
178 represented previous sampling work^{32,33} and new sampling that covered all known existing
179 populations.

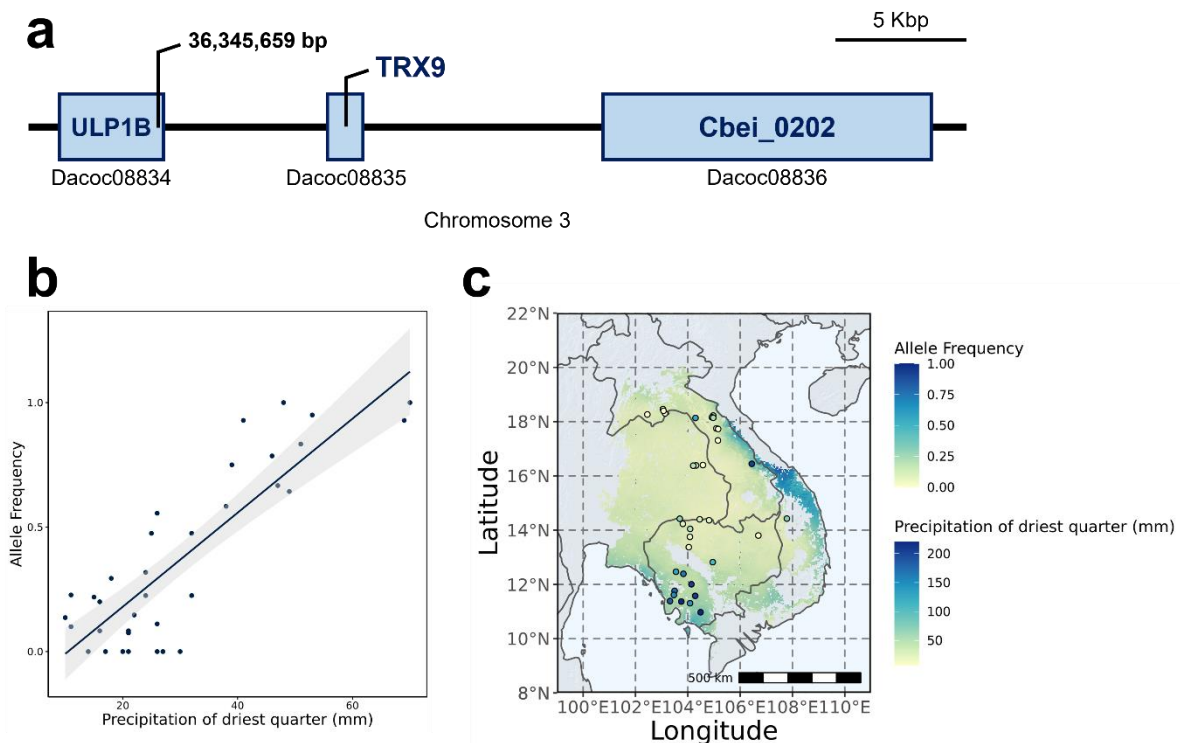
180 We employed the sparse non-negative matrix factorisation (sNMF) algorithm to
181 determine the optimal number of ancestral populations (K) for *D. cochinchinensis* and *D.*
182 *oliveri* as 13 and 14 respectively (Supplementary Figure 3, Supplementary Figure 4,
183 Supplementary Figure 5). These results were much higher than the previous estimation of K
184 = 5 – 9 for the same species using nine microsatellite markers and 19 SNPs^{32,33}. The analysis
185 revealed a highly resolved hierarchical genetic structure for both species and distinct
186 population clusters around the Cardamon Mountains in southwest Cambodia and in northern
187 Laos. Our calculation gave a larger genomic inflation factor (λ) in *D. cochinchinensis* (range
188 from 0.071 (evapotranspiration) to 0.25 (precipitation of driest quarter), mean of 0.13,
189 standard deviation of 0.049) than that in *D. oliveri* (range from 0.038 (evapotranspiration) to

190 0.081 (mean diurnal range), mean of 0.056, standard deviation of 0.016 (Supplementary
191 Table 8).

192 The numbers of SNPs found to be adaptive for at least one of the environmental
193 variables were 20,373 (11.3%) and 6,953 (3.59%) in *D. cochinchinensis* and *D. oliveri*
194 respectively ($|Z\text{-value}| > 2$ & $Q\text{-value} < 0.01$), after correcting for population structure
195 (optimal K) and genomic inflation (Supplementary Figure 6, Supplementary Figure 7,
196 Supplementary Table 9). Relatively few SNPs were associated with all or many
197 environmental variables; 4 SNPs were associated with 11 out of 13 variables tested in *D.*
198 *cochinchinensis*, and 46 SNPs were associated with all 12 variables in *D. oliveri*. These
199 findings revealed the complex and polygenic nature of environmental adaptation, where
200 multiple forces of natural selection can act together via different environmental cues and
201 affect overlapping loci.

202 In *D. cochinchinensis*, ‘precipitation in the driest quarter’ was the environmental
203 variable (wc2.1_30s_bio_17) and the strongest gene-environmental association with a SNP
204 on chromosome 3 at position 36,345,659 (LFMM $Z = 6.07237$, $Q = 4.77e-29$). The SNP was
205 located within the gene Dacoc08834, a homologue of the Ubiquitin-like-specific protease 1B
206 ULP1B. The highest allele frequencies of this SNP were found in the southwest of Cambodia
207 with the highest precipitation of the driest quarter (Figure 2). ULP1B is one of the ubiquitin
208 like-specific proteases that mediate the maturation and deconjugation of a small ubiquitin-
209 like modifier (SUMO) from target proteins as part of post-translational modification³⁴. The
210 SUMO process in plants has been shown to regulate stress responses including to drought,
211 heat, salinity, and pathogens^{35–37} and timing of flower initiation³⁸, which might explain the
212 strong association with the drought stress associated with the said environmental factor. In an
213 analysis of transcriptomes from 6 *Dalbergia* species, ubiquitin-related proteins were found to

214 be overrepresented compared to other legumes²⁷. Taken together, these observations suggest
215 that ubiquitin-related proteins have a role in *Dalbergia* adaptation to water assimilation.



216

217 **Figure 2.** (a) The most significant gene-environment association at 36,346,659 bp on chromosome 3, within the *Dacoc08834*
218 gene and upstream of *Dacoc08835* and *Dacoc08836* genes, which are homologues of *ULP1B*, *TRX9*, and *Cbei_0202*
219 respectively. (b) and (c) Correlation between allele frequency and *wc2.1_30s_bio_17* (Precipitation of driest quarter) for
220 this locus.

221 By contrast, the strongest association in *D. oliveri* was between precipitation of the
222 wettest quarter (*wc2.1_30s_bio_16*), and a SNP on the scaffold *Daoli_0035* at the position
223 107,725 (LFMM $Z = 6.1895$, $Q = 6.36e-102$). The locus was 3,254 bp upstream of a
224 predicted gene model *Daoli32516* and 5,010 bp downstream of the gene *Daoli32517*, a
225 homologue of *tatC*-like protein *YMF16*.

226

227 Differential adaptation related to temperature and precipitation

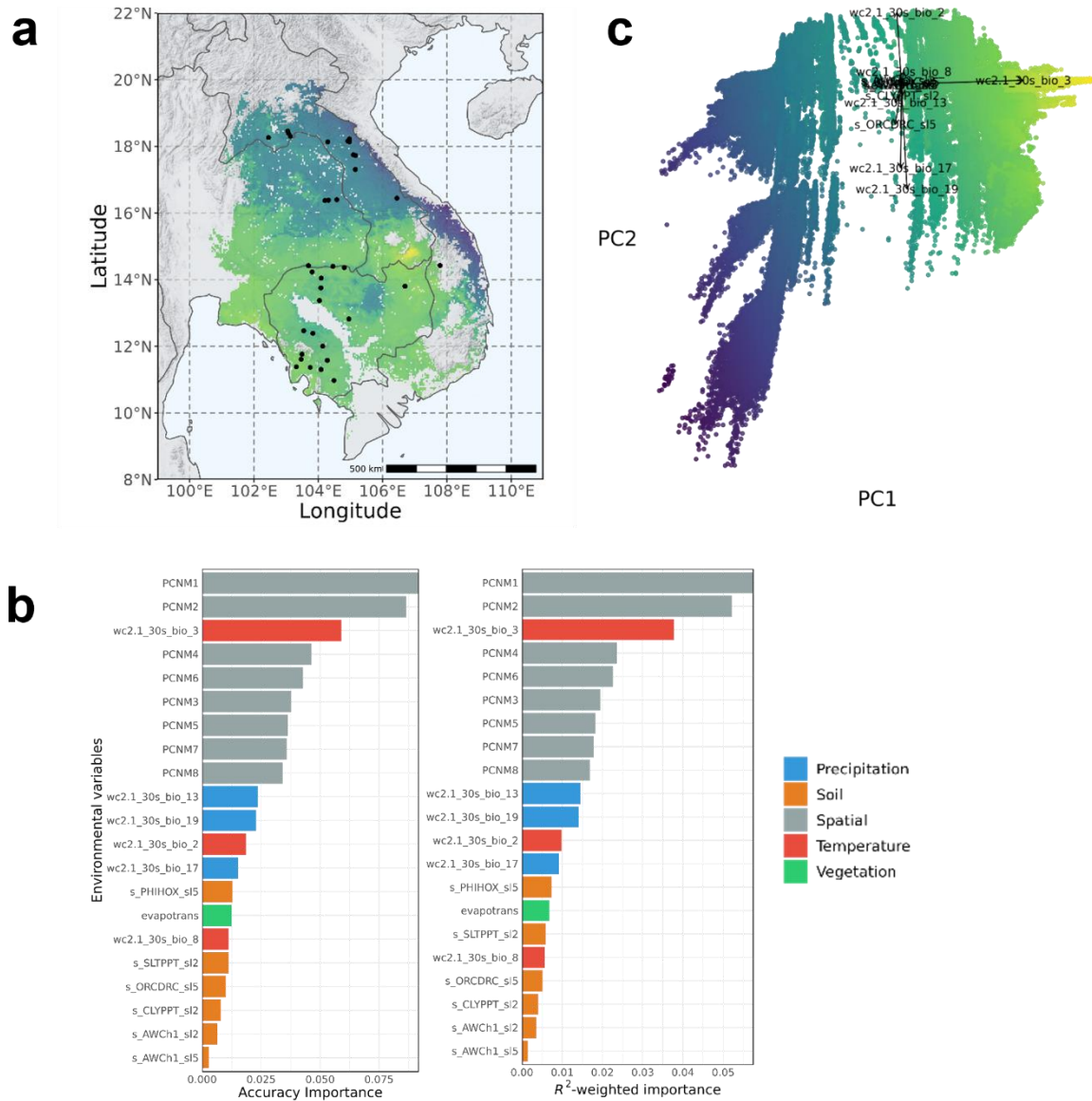
228 Isothermality (*wc2.1_30s_bio_3*) was identified as the most important overall driver
229 of both neutral and adaptive genomic variation among non-spatial environmental variables in
230 *D. cochinchinensis*, based on our gradient forest (GF) model (Figure 3, Supplementary

231 Figure 8a), in contrast to ‘precipitation of the wettest quarter’ (wc2.1_30s_bio_16) in *D.*
232 *oliveri* (Figure 4, Supplementary Figure 8b). Spatial variables, as principal coordinates of a
233 neighbourhood matrix (PCNM), were the most important variables that explained both
234 neutral and adaptive genomic variation, which was unsurprising given strong isolation by
235 distance was known in these species³² and environmental adaptation only affects a small
236 portion of the genome³⁹. Soil factors were among the lowest ranked variables for gene-
237 environment associations for both species. We observed different patterns of geographic
238 variation in *D. cochinchinensis* and *D. oliveri* when fitting the GF models across their native
239 ranges. *D. cochinchinensis* had strong differentiation between North and South populations at
240 around 16°N, that was mainly driven by isothermality (wc2.1_30s_bio_3) as seen in the PCA
241 loadings. On the other hand, *D. oliveri*’s major differentiation was between coastal and inland
242 areas, driven by both precipitation of the wettest quarter (wc2.1_30s_bio_16) and mean
243 diurnal range (wc2.1_30s_bio_2). The eastern coastal areas in Vietnam showed particularly
244 strong differences in environmental associations with adaptive variation and neutral variation
245 for both *D. cochinchinensis* and *D. oliveri* (Figure 5).

246

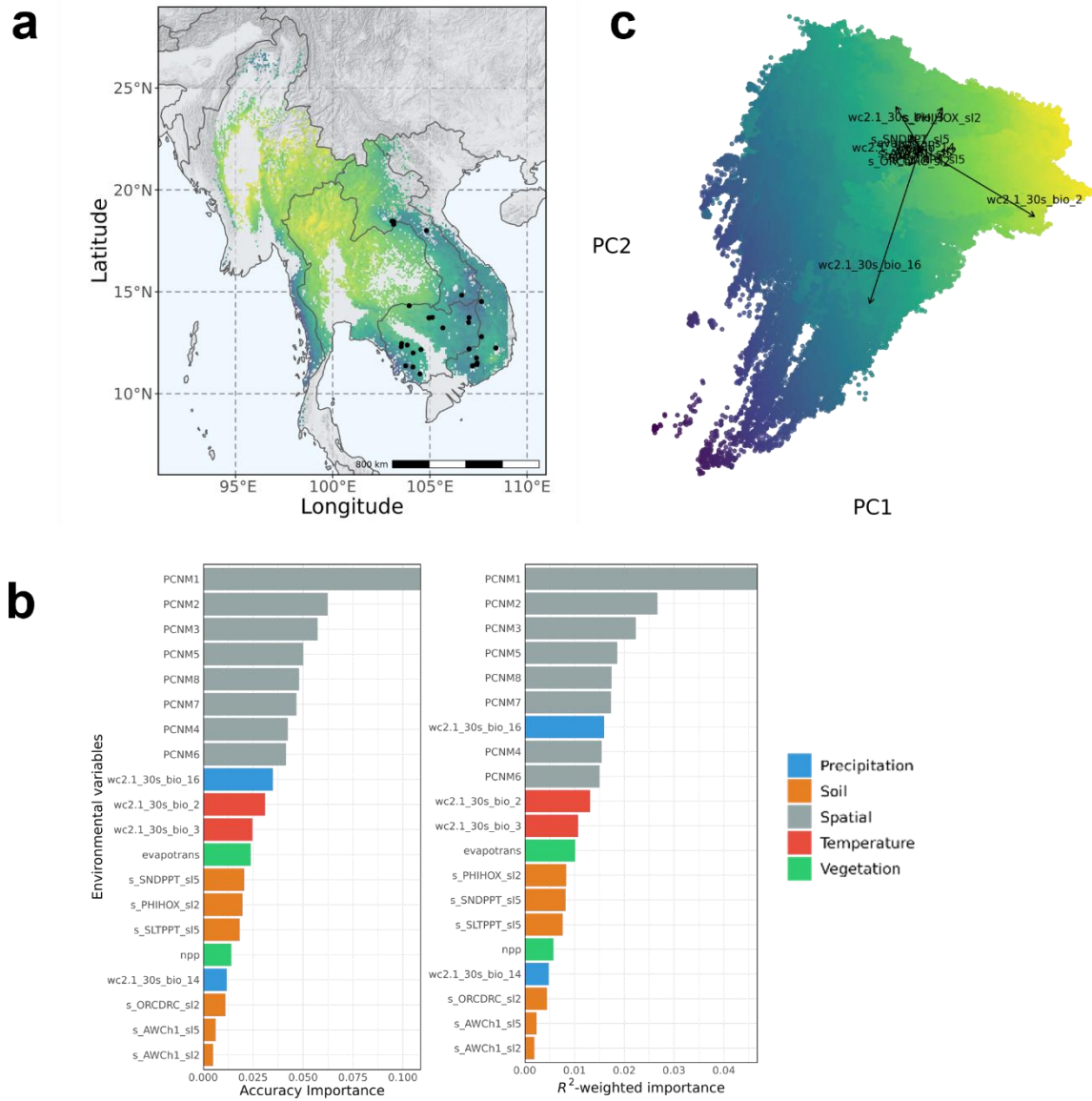
247

248



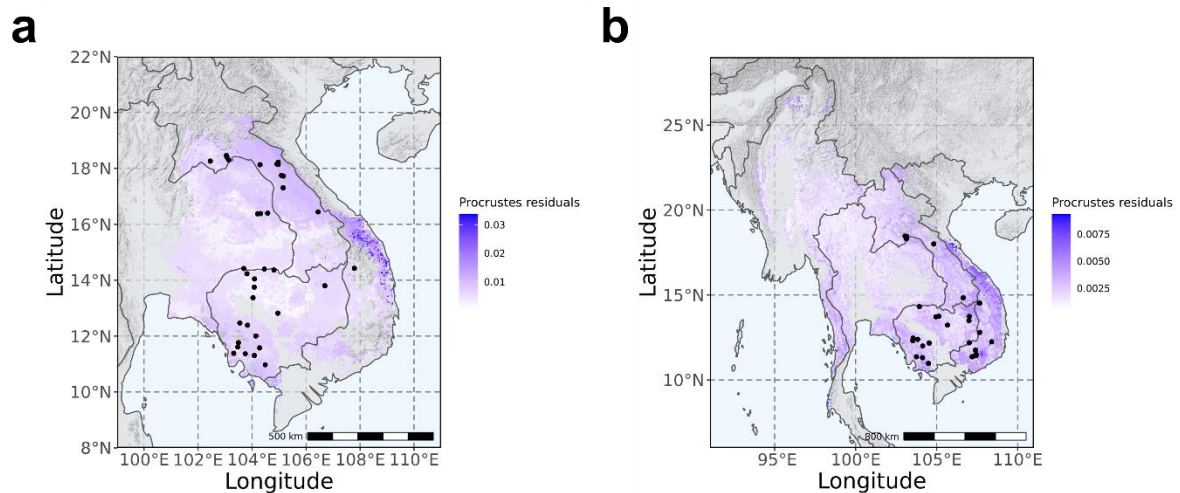
249

250 **Figure 3.** (a) Adaptive genomic variation across the species range predicted by GF model for *D. cochinchinensis*, visualised
 251 using the first two principal axes from the PCA. (b) Accuracy and R^2 -weighted importance for environmental predictor
 252 variables which explained adaptive genomic variation (adaptive SNPs) by the GF model. (c) Principal component analysis
 253 (PCA) of the adaptive genomic variation predicted by the GF model across the species range. Loadings are the
 254 environmental factors.



255

256 **Figure 4.** (a) Adaptive genomic variation across the species range predicted by GF model for *D. oliveri*, visualised using the
 257 first two principal axes from the PCA. (b) Accuracy and R^2 -weighted importance for the environmental predictor variables
 258 which explained the adaptive genomic variation (adaptive SNPs) by the GF model. (c) Principal component analysis (PCA)
 259 of the adaptive genomic variation predicted by the GF model across the species range. The loadings are the environmental
 260 factors.



261

262 *Figure 5. Procrustes residuals between neutral and adaptive gene-environmental associations for (a) D. cochinchinensis*
263 *and (b) D. oliveri.*

264 We compared the allelic frequency turnover functions of the neutral and adaptive
265 genomic variation for each environmental predictor variable. Adaptive genomic variation was
266 significantly more strongly associated with environmental gradients than neutral variation
267 (Supplementary Figure 9). There was only one exception, where available soil water capacity
268 at a depth of 60 cm (s_AWCh1_sl5) was near-zero but of similar importance in explaining
269 neutral and adaptive variation, regardless of the environmental gradient.

270 When exposed to drought stress under controlled conditions, *D. cochinchinensis* was
271 more anisohydric than *D. oliveri*, which means that *D. cochinchinensis*, as a pioneering
272 species with faster growth, optimises carbon assimilation and better tolerates reduced water
273 availability³. *D. oliveri* is often found in moist areas and along streams and rivers⁴⁰, and the
274 morphological characteristics of its seeds suggest that secondary dispersal by water is likely³².
275 This could explain how isothermality, which is a useful metric in tropical environments⁴¹ and
276 shown to influence plant height growth⁴², had a dominant effect in the adaptive variation only
277 in *D. cochinchinensis*. Pioneering species maximise height growth in early successional
278 habitats to meet their light requirements⁴³, consistent with the observation of higher
279 photosynthetic pigment levels in *D. cochinchinensis*³. On the other hand, the effect of

280 precipitation of the wettest quarter could act on selection in seed dispersal and survival in *D.*
281 *oliveri* in the wet season. Temperature and precipitation, and their variability such as
282 isothermality⁴⁴ have been widely reported as the most important drivers shaping patterns of
283 productivity and adaptation in tree species across the world^{45–47}.

284 To fill the current gaps in existing conservation actions, populations that are
285 underrepresented but display distinct adaptive variation should be prioritised to avoid the
286 potential loss of unique genetic diversity. Populations at the edge of the species ranges should
287 be prioritised based on our findings on adaptive variation showing their distinct allelic
288 frequencies and adaptation; however, they are currently underrepresented in conservation
289 efforts and existing protected area networks. Importantly, hotspots of differential adaptive
290 variation near the edges of species ranges are shared between *D. cochinchinensis* and *D.*
291 *oliveri*. This observation reinforces the role of marginal populations in preserving
292 evolutionary potential for range expansion and persistence due to their adaptation to distinct
293 environmental conditions⁴⁸.

294

295 **Genomic vulnerability under different climate change scenarios**

296 Genetic offset in the form of Euclidean distance represented the mismatch between
297 current and future gene-environment association, which was modelled over five general
298 circulation models (GCMs), namely MIROC6, BCC-CSM2-MR, IPSL-CM6A-LR, CNRM-
299 ESM2-1, MRI-ESM2-0, under WCRP CMIP6 (Supplementary Figure 10). For both
300 *Dalbergia* species, genetic offset generally increased over time ($P = 2.71e-10$) and shared
301 socioeconomic pathway ($P = 4.54e-14$), which implies increased carbon emission (Figure 6a,
302 Supplementary Table 10). However, *D. cochinchinensis* shows a significantly larger increase
303 in genetic offset over time compared to *D. oliveri* ($P = 0.025$), suggesting that *D.*
304 *cochinchinensis* is more susceptible to any mismatch of current genotypes and future climate.

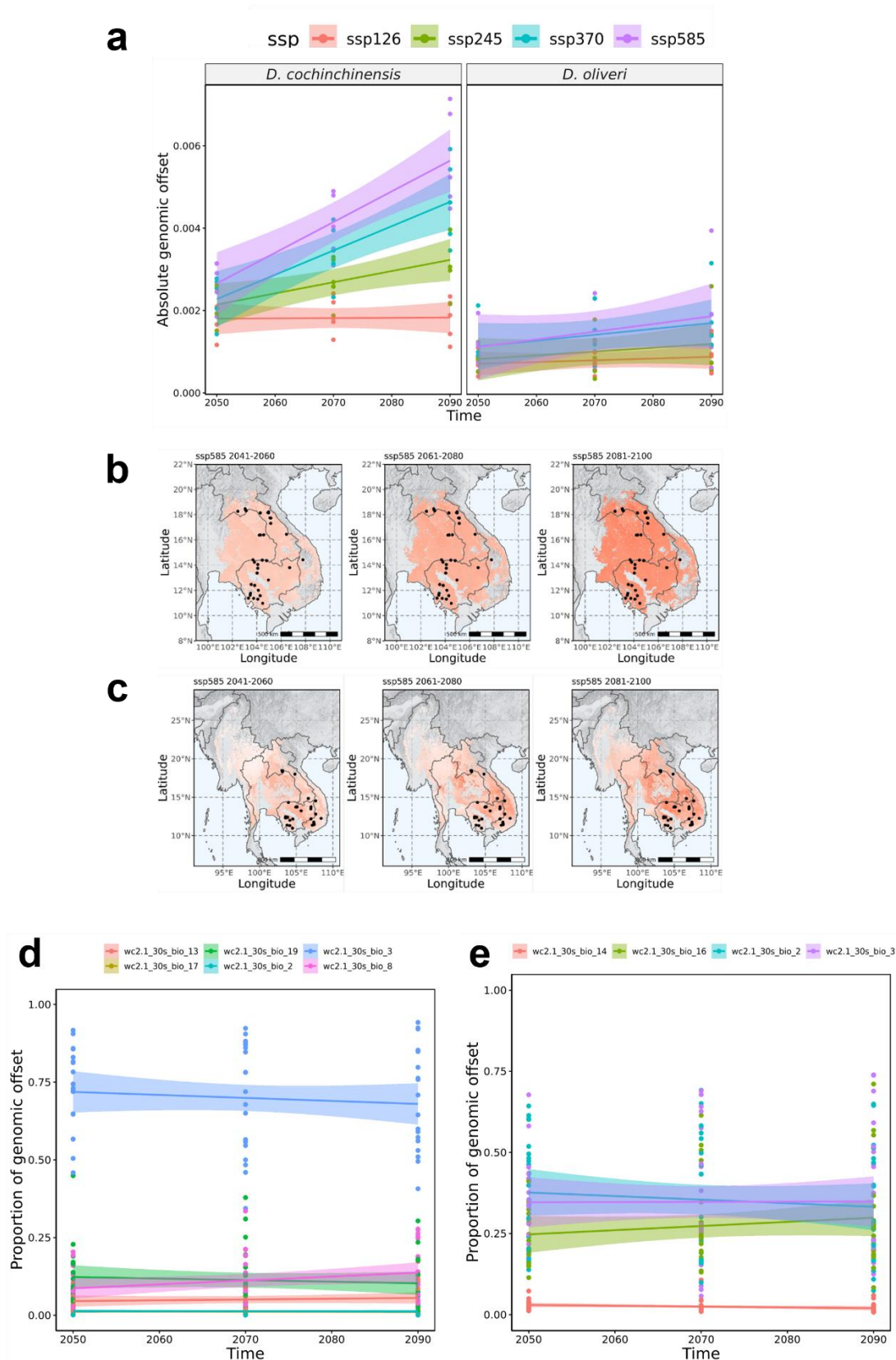
305 The geographic patterns of genetic offset also differed between the two species: *D.*
306 *cochinchinensis* had an increasing offset across the entire range, while *D. oliveri* had a
307 distinctly high offset in the southeast part of the range (Figure 6b–c). The variation in
308 genomic offset between two species was mainly driven by the strong association with
309 isothermality (*wc2.1_30s_bio_3*) in *D. cochinchinensis*, as demonstrated in the GF model, as
310 it contributed to ~75% of the genomic offset on average (Figure 6d). Isothermality had a
311 smaller effect (~35%) in *D. oliveri* (Figure 6e).

312 Our prediction contrasts with a separate sensitivity-and-exposure modelling study
313 which predicted that *D. oliveri* is likely to be slightly more vulnerable to climate change by
314 2055 (2041–2070 period) than *D. cochinchinensis*¹². It used growth rate and seed weight as
315 proxy traits, predicting that both species have equally high sensitivity to climate change, but
316 that *D. oliveri* is more exposed to the threat. Our findings predict that the dominant
317 environment factor of isothermality could give more weight to the species' vulnerability. As
318 discussed, isothermality is likely to affect the productivity and growth in pioneering species
319 like *D. cochinchinensis* more than later successional species like *D. oliveri*. Our work
320 supports that isothermality and other temperature variation factors will serve as more reliable
321 indicators to predict the climate response of *D. cochinchinensis* and encourages further
322 studies of this response, such as greenhouse or common garden experiments to validate the
323 prediction with empirical data.

324 The different geographical patterns of genomic vulnerability support species-specific
325 recommendations in conservation and restoration. While climate change is likely to affect *D.*
326 *cochinchinensis* evenly across its range, greater attention is needed on the representation of
327 adaptive variation in germplasm collection and conservation units; sampling should target
328 edge populations in particular as they show potential signals of local adaptation, where the
329 environmental associations between adaptive and neutral variation are the greatest. By

330 contrast, we recommend targeting hotspots of vulnerability in *D. oliveri*, especially around
331 the borders between Cambodia, Laos, Vietnam, and Thailand, to improve conservation
332 efforts.

333 In a rapidly changing environment, forest trees either persist through migration or
334 phenotypic plasticity, or will extirpate⁴⁵ when environmental change outpaces adaptation
335 potential. The spatially explicit model of genomic vulnerability helps to develop conservation
336 decisions balancing between *in situ* adaptation and assisted migration, as populations with
337 lower vulnerability are likely to persist through adaptation⁴⁹.

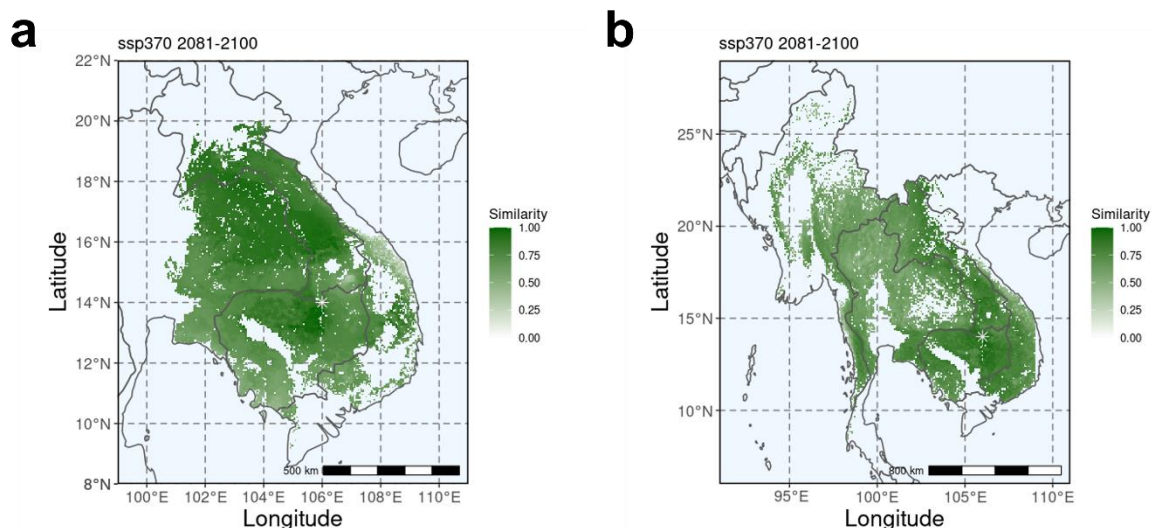


338

339 **Figure 6.** (a) Absolute genomic offset of gene-environment association, quantified as the Euclidean distance, of *D.*
 340 *cochinchinensis* and *D. oliveri* in 4 SSPs (126, 245, 370, and 585) over three bidecades (2041–2060, 2061–2080, 2081–
 341 2100) averaged across five GCMs (BCC-CSM2-MR, CNRM-ESM2-1, IPSL-CM6A-LR, MIROC6, MRI-ESM2-0). Scaled
 342 genomic offset across the range of (b) *D. cochinchinensis* and (c) *D. oliveri*, using SSP585 between 2041 and 2060 as an
 343 example. Proportion of genomic variation explained by environmental variables in (d) *D. cochinchinensis* and (e) *D. oliveri*.

344 **Genomic model-enabled assisted migration and restoration**

345 We developed *seedeR*, an open-source web application that is freely available from
346 <https://trainingidn.shinyapps.io/seedeR/>, where users can input the species (*D.*
347 *cochinchinensis* or *D. oliveri*), shared socioeconomic pathways (SSP), time period, and
348 geographical coordinates of the target restoration or planting site. With these inputs, *seedeR*
349 predicts the genomic similarity between a current germplasm source and target site from
350 allelic frequency turnover functions and genetic offset and projects them onto the species
351 range. We demonstrate the utility of *seedeR* for a hypothetical target restoration site (106° N,
352 14° E) in northeast Cambodia for both *D. cochinchinensis* and *D. oliveri*, under the future
353 climate scenario of SSP370 between 2081 and 2100 (Figure 7). In both predictions, the
354 genomic similarity was the highest at proximity to several hundreds of kilometres and
355 decreased when further away. Commonly, coastal regions in northeast Vietnam, which were
356 predicted to have the strongest local adaptation in both species, showed a lower genomic
357 similarity. The geographical scale of suitable seed sources has an important implication as too
358 many forest landscape projects collect seeds from very close (a few kilometres) to restoration
359 sites to feed the “local is best” paradigm⁵⁰, while our predictions showed otherwise. It is also
360 important to note that local tree populations in landscapes in need of restoration are often
361 degraded and have low genetic diversity. Genetic quality of seed should be ensured by
362 collecting seed from large populations and many unrelated trees, even if this means collecting
363 from trees at distances much further from the target restoration site.



364

365 **Figure 7.** Genomic similarity (scaled between 0, most dissimilar, and 1, most similar) between a hypothetical future
366 restoration site (106° N, 14° E) and the current potential germplasm sources under the future climate scenario of SSP370
367 between 2081 and 2100 for (a) *D. cochinchinensis* and (b) *D. oliveri* predicted on *seedeR*
368 (<https://trainingidn.shinyapps.io/seedeR/>).

369 Matching seed sources and restoration sites remains one of the keys for effective
370 conservation and restoration⁵¹, in line with the importance of adaptive variation and potential
371 in genetic materials. Our genome-enabled prediction tool considers the future climate of
372 restoration sites, which in turn will greatly influence the future resilience and productivity of
373 these species. In the case of maladaptation and extirpation due to environmental change⁵²,
374 when the classical preference for local provenance may no longer hold, deliberate transfer of
375 germplasm along climate gradients may be necessary⁵³. Especially in the case of *Dalbergia*,
376 when many local populations have extirpated or are very small in size, and large
377 environmental association was predicted, assisted migration based on admixture and
378 predictive provenancing are deemed more appropriate for the species to facilitate adaptation
379 of the populations under climate change⁵⁴. Genetic materials from regions with strong
380 adaptive genomic variation, such as coastal Vietnam, can be moved to suitable regions using
381 the *seedeR* prediction to facilitate gene flow and maintain unique genetic components of the
382 population by admixture⁵³. Hotspots of vulnerable populations such as those in northern
383 Cambodia are suitable to be moved to new suitable areas to prevent loss of genetic diversity.

384 The *seedeR* application helps to visualize these spatially explicit predictive models of
385 genomic vulnerability and match, which are most useful to frontline practitioners and
386 managers⁵⁵. Not only can it inform conservation and management strategies, but by
387 simplifying the analytical pipelines through a user-friendly platform, it will also directly
388 reduce the gap between conservation and genomics; a challenge faced for dissemination of
389 genomic knowledge⁵⁶.

390

391 **Narrowing the gap between conservation and genomics**

392 Our study characterises range-wide gene-environment association in two sympatric
393 endangered species, *D. cochinchinensis* and *D. oliveri*, for which there was virtually no prior
394 knowledge on adaptability. Building on previous understanding of their different
395 physiologies, we demonstrate their differential adaptive characteristics, which point to
396 species-specific implications for their conservation. These findings on differential genomic
397 adaptation between sympatric species sheds novel understanding on tropical forests, which in
398 particular harbour many threatened species, at risk from threats associated with climate
399 change.

400 We show how genomic technologies can directly support rapid decision-making and
401 conservation activities. The separation between scientific and conservation communities
402 represents a long-standing challenge, such that advances in scientific research and
403 specifically genomic technologies are often inaccessible to the conservation side, which
404 hinders translational science^{57,58}. Through engagement with diverse stakeholders and
405 conservation activities, we were strongly motivated to deliver the results of this study in a
406 user-friendly (e.g. *seedeR*) and spatially explicit manner that can be integrated with ongoing
407 conservation work.

408 **Methods**

409 *Plant materials and sample preparation for genome assemblies*

410 Dried seeds of *Dalbergia cochinchinensis* and *D. oliveri* were collected from the
411 Bolikhamxay, Khamkend, Laos, and Phnom Penh, Cambodia in 2018 by their forestry
412 authorities respectively. We germinated the seeds in a greenhouse at 30°C with 16L/8D
413 photoperiod. Leaf tissues were harvested from a selected 1-year-old individual for each
414 species and ground in liquid nitrogen with a mortar and pestle.

415 High-molecular-weight genomic DNA was extracted from the reference individual
416 with Carlson lysis buffer (100 mM Tris-HCl, pH 9.5, 2% CTAB, 1.4 M NaCl, 1% PEG 8000,
417 20 mM EDTA) followed by purification using the QIAGEN Genomic-tip 500/G. The
418 quantity and quality of genomic DNA were determined with NanoDrop 2000 (Thermo,
419 Wilmington, United States) and Qubit 4 (Thermo Fisher Scientific, United Kingdom). DNA
420 integrity was preliminary assessed with a 0.4% agarose gel against a NEB Quick-Load® 1 kb
421 Extend DNA Ladder. A DNA sample passed the quality check only when a single band could
422 be mapped near a lambda DNA band (~ 48.5 kb).

423

424 *Genomic sequencing and assembly of D. cochinchinensis*

425 For Oxford Nanopore sequencing, 9 µg of extracted DNA was size-selected using the
426 Circulomics Short Read Eliminator XL Kit (Maryland, United States) to deplete fragments <
427 40 Kbp. Three libraries were prepared each starting from 3 µg of size-selected DNA was
428 used in each library preparation with the Oxford Nanopore Technologies Ligation
429 Sequencing Kit (SQK-LSK110). The libraries were sequenced on two R10.3 (FLO-109D)
430 flow cells on a GridION sequencer for ~ 72 hours. Real-time basecalling was performed in
431 MinKNOW release 19.10.1. Raw reads with Phred score lower than 8 were filtered.

432 For PacBio sequencing, DNA samples were sent to the Genomics & Cell
433 Characterization Core Facility at the University of Oregon for DNA library preparation and
434 sequencing. Throughout the sample preparation, the quality of DNA was assessed using
435 Fragment Analyzer 1.2.0.11 (Agilent, United States). 20 µg of unsheared genomic DNA was
436 used for library preparation using the SMRTbell Express Template Prep Kit 2.0 (Pacific
437 Biosciences, United States). The library was size selected using the BluePippin system (Sage
438 Science, United States) at 45 kb and then sequenced on a single SMRT 8M cell on a Sequel II
439 System (2.0 chemistry) using the Continuous Long-Read Sequencing (CLR) mode with a
440 movie time of 30 hours.

441 For Hi-C sequencing, we harvested 0.5 g of fresh leaf from the same reference
442 individual and immediately cross-linked the finely chopped tissue in 1% formaldehyde for 20
443 minutes. The cross-linking was then quenched with glycine (125 mM). The cross-linked
444 samples were ground in liquid nitrogen with a mortar and pestle and shipped to Phase
445 Genomics (Seattle, USA) for library preparation and sequencing. The Hi-C library was
446 prepared with the restriction enzyme DpnII, proximity-ligated, and reverse-crosslinked using
447 Proximo Hi-C Kit (Plant) v2.0 (Phase Genomics, Seattle, USA). The library was sequenced
448 on a HiSeq4000 for ~300 M 150-bp paired-end sequencing.

449

450 ***Genomic sequencing of *D. oliveri****

451 For Nanopore sequencing, the same protocol and procedure were used as for *D.*
452 *cochinchinensis* (see above).

453 For Pore-C sequencing, the library was prepared with the protocol and reagents
454 described by Belaghzal et al.⁵⁹ with minor modifications. We harvested 2 g of fresh leaf from
455 the same reference individual as for the Nanopore library and immediately cross-linked the
456 finely chopped tissues in 1% formaldehyde for 20 minutes. The cross-linking was quenched

457 with 125 mM glycine for 20 minutes and then the samples were ground in liquid nitrogen
458 with a mortar and a pestle. Cell nuclei were isolated with a buffer containing 10 mM Trizma,
459 80 mM KCl, 10 mM EDTA, 1 mM spermidine trihydrochloride, 1 mM spermine
460 tetrahydrochloride, 500 mM sucrose, 1% (w/v) PVP-40, 0.5% (v/v) Triton X-100, and 0.25%
461 (v/v) β -mercaptoethanol, and then passed through a 40 μ m cell strainer. The suspension was
462 centrifuged at 3,000 g, according to the estimated genome size of \sim 700 Mbp. Chromatin was
463 denatured with the restriction enzyme NlaIII at a final concentration of 1 U/ μ L (New England
464 Biolabs, United Kingdom) at 37°C for 18 hours. The enzyme was heat-denatured at 65°C for
465 20 minutes at 300 rpm rotation in a thermomixer. Proximity ligation, protein degradation,
466 decrosslinking, and DNA extraction were performed according to the original Belaghzal
467 protocol. The Pore-C library was prepared with the Oxford Nanopore Technologies Ligation
468 Sequencing Kit (SQK-LSK110), then sequenced on two R10.3 (FLO-109D) Nanopore flow
469 cells on a GridION sequencer for \sim 72 hours. The flow cell was washed once every 24 hour
470 with the Flow Cell Wash Kit (EXP-WSH003).

471

472 ***Assembly pipelines***

473 Raw reads shorter than 500 bp were filtered. Due to the heterozygous nature of the
474 wild individual, we assembled the sequences with Canu 2.1.1 using the options
475 “corOutCoverage=200 correctedErrorRate=0.16 batOptions=-dg 3 -db 3 -dr 1 -ca 500 -cp
476 50”. We then used purge_haplotigs v1.1.1 to collapse the assembly by separating the primary
477 assembly and haplotigs.

478 Hi-C reads (for *D. cochinchinensis*) were mapped to the draft genome assembly using
479 hicstuff 2.3.2⁶⁰ to generate the contact matrix, which was then used to scaffold and polish the
480 assembly using instaGRAAL 0.1.2⁶¹ with default options to produce the final assembly
481 Dacoc 1.4 after removing contamination.

482 Pore-C reads (for *D. oliveri*) were mapped to the draft genome assembly and used to
483 generate contact map with the Pore-C-Snakemake ([https://github.com/nanoporetech/Pore-C-](https://github.com/nanoporetech/Pore-C-Snakemake)
484 [Snakemake](#)) and produce a merged_nodups (.mnd) file, which contains a duplicate-free list of
485 paired alignments from the Pore-C reads to the draft assembly. The draft assembly and the
486 merged_nodups file were used for scaffolding in 3D-DNA (version 180419) and produce the
487 final genome Daoli 0.3.

488 To validate the scaffold arrangement, Daoli 0.3 was aligned to that of *D.*
489 *cochinchinensis* (Dacoc 1.4) using minimap2 and D-GENIES⁶² to produce a dot plot for
490 visualising similarity, repetitions, breaks, and inversions, with a minimum identity of 0.25.

491

492 ***De novo repeat library***

493 A *de novo* repeat library was constructed using RepeatModeler 2.0.1⁶³, which
494 incorporated RECON 1.08⁶⁴, RepeatScout 1.0.6⁶⁵, and TRF 4.0.9⁶⁶ for identification and
495 classification of repeat families. We then used RepeatMasker 4.1.1⁶⁷ to mask low complex or
496 simple repeats only (“-noint”). A *de novo* library of long terminal repeat (LTR)
497 retrotransposons was constructed on the simple-repeat-masked genome using LTRharvest⁶⁸
498 and annotated with the GyDB database and profile HMMs using LTRdigest⁶⁹ module in the
499 genomertools 1.6.1 pipeline. Predicted LTR elements with no protein domain hits were
500 removed from the library. We applied the RepeatClassifier module in RepeatModeler to
501 format both repeat libraries. We merged the libraries together and clustered the sequences
502 that were $\geq 80\%$ identical by CD-HIT-EST 4.8.1⁷⁰ (“-aS 80 -c 0.8 -g 1 -G 0 -A 80”) to
503 produce the final repeat library.

504

505 ***Gene models and annotation***

506 Filtered mRNA-sequencing data for *D. cochinchinensis* (50.5 Gbp) and *D. oliveri*
507 (54.4 Gbp) from a previous project²⁷ (NCBI Bioproject: PRJNA593817) were aligned against
508 the genome assembly using STAR v2.7.6 and assembled using the genome-guided mode of
509 Trinity v2.13.2. Protein sequences were obtained from *Arabidopsis thaliana* (Araport11)⁷¹
510 and *Arachis ipaensis* (Araip1.1)⁷². After soft-masking the genome with the *de novo* repeat
511 library using RepeatMasker (Dfam libraries 3.2), the transcript and protein evidences were
512 used to produce gene models using MAKER 3.01.03⁷³. The MAKER pipeline was iteratively
513 run for two more rounds to produce the final gene models. In between each run of MAKER,
514 the gene models were used to train the *ab initio* gene predictors SNAP (version 2006-07-28)⁷⁴
515 and AUGUSTUS 3.3.3⁷⁵ which were used in the MAKER pipeline. tRNA genes were
516 predicted with tRNAscan-SE 1.3.1⁷⁶. The quality of the gene models was assessed with two
517 metrics: the annotation edit distance (AED) in MAKER 3.01.03⁷³ and the BUSCO score
518 (v5.1.2)⁷⁷.

519

520 ***Population sampling***

521 We obtained a collection of 435 and 331 foliage samples of *Dalbergia*
522 *cochinchinensis* and *D. oliveri* from 35 and 28 localities across their native range
523 (Supplementary Table 11). These samples were a combination of those collected in a
524 previous study³² and newly between 2019 and 2020. Genomic DNA was purified using a two-
525 round modified CTAB protocol (2% CTAB, 1.4 M NaCl, 1% PVP-40, 100 mM Tris-Cl pH
526 8.0, 20 mM EDTA pH 8.0, 1% 2-mercaptoethanol) with sorbitol pre-wash (0.35 M Sorbitol,
527 1% PVP-40, 100 mM Tris-Cl pH 8.0, and 5 mM EDTA pH 8.0) as the samples were rich in
528 polyphenols and polysaccharides⁷⁸. Genomic DNA was treated with 5 µL RNase (10
529 mg/mL). Quality and quantity of the genomic DNA were assessed using NanoDrop One

530 (Thermo, Wilmington, United States) and Qubit dsDNA BR Assay kit on Qubit 4 (Thermo,
531 Wilmington, United States) respectively.

532

533 ***Genotyping-by-sequencing (GbS)***

534 DNA samples were normalised to 200 ng suspended in 10 μ L water and sent to the
535 Genomic Analysis Platform, Institute of Integrative and Systems Biology, Université Laval
536 (Quebec, Canada) for GbS library preparation. DNA was digested with a combination of
537 restriction enzymes PstI/NsiI/MspI, ligated with barcoded adapter, and pooled to
538 equimolarity. The pooled library was amplified by PCR and sequenced on a Illumina
539 NovaSeq6000 S4 with paired-end reads of 150 bp at the G enome Qu ebec Innovation Centre,
540 (Montreal, Canada).

541

542 ***Variant calling***

543 DNA sequence variant calling was done with the Fast-GBS v2.0 pipeline⁷⁹: Illumina
544 raw reads were demultiplexed with Sabre 1.0⁸⁰ and trimmed with Cutadapt 1.18⁸¹ to remove
545 the adaptors. Trimmed reads shorter than 50 bp were discarded. Reads were aligned against
546 the Dacoc 1.0 genome (Hung et al., unpublished) and the Daoli 0.1 genome using BWA-
547 MEM 0.7.17⁸². The SAM alignment files were converted to BAM format and indexed using
548 SAMtools 1.9⁸³. Variant calling was performed in Platypus⁸⁴ and variants were filtered with
549 proportion of missing data of 0.2 and minimum allele frequency (MAF) of 0.01 using
550 VCFtools 0.1.16⁸⁵. Missing genotype was imputed using Beagle 5.2. Finally, linkage
551 equilibrium among SNPs was detected using BCFtools 1.9⁸³, and one SNP was removed from
552 all SNP pairs with $r^2 > 0.5$ in a genomic window of 5 Kbp.

553

554 ***Environmental heterogeneity characterisation***

555 Environmental data were obtained from different sources (34 variables in total,
556 Supplementary Table 12) and represented different measurers of temperature, precipitation,
557 their seasonality, soil, elevation, and vegetation. We calculated a correlation matrix across the
558 sampling localities and highly inter-correlated variables (pairwise correlation coefficient $| >$
559 0.7) were detected. For each inter-correlated variable pair, the one variable with the largest
560 mean absolute correlation across all variables was removed.

561

562 ***Population genetic structure and identification of putatively adaptive loci***

563 Population genetic structure was assessed with sparse non-negative matrix
564 factorisation (sNMF) to estimate the number of discrete genetic clusters (K)⁸⁶. The sNMF
565 was run for 10 repetitions for each value of K from 1 to 15 with a maximum iteration of 200.
566 The optimal K was selected based on the lowest cross-entropy value from the sNMF run, or
567 where the value began to plateau. Admixture plots were drawn for $K = \{2, 4, 8, \text{optimal } K\}$.
568 Population structure-based outlier analysis was also conducted with sNMF, in which outlier
569 SNPs that are significantly differentiated among populations, based on estimated F_{ST} values
570 from the ancestry coefficients obtained from sNMF⁸⁷, were obtained and mapped on the 10
571 putative chromosomes for *D. cochinchinensis* or the 16 longest scaffolds for *D. oliveri* in a
572 Manhattan plot.

573 We used latent factor mixed modelling (LFMM) to test for significant associations
574 between environmental variables and SNP allele frequencies. The optimal K obtained from
575 the sNMF was used in LFMM to correct for the neutral genetic structure. LFMM was run for
576 3 repetitions with a maximum iteration of 1,000 and 500 burn-ins. Z -scores were obtained for
577 all repetitions for each environmental variable, and then the median was taken for each SNP.
578 Next, the genomic inflation factor λ , defined as the observed median of Z -scores divided by

579 the expected median of the chi-squared distribution for each environmental association⁸⁸, was
580 calculated to calibrate for P -values:

$$\lambda = \frac{\text{median}(Z^2)}{\chi_1^2(0.5)}, \text{ such that } P_{\text{adjusted}} = \chi_1^2\left(\frac{Z^2}{\lambda}\right).$$

581

582 The calibration was then inspected on a histogram of P -values for each environmental
583 association. Finally, multiple testing was corrected with the Benjamini and Hochberg method
584 to obtain Q -values.

585 The sNMF and LFMM calculations were performed in R 4.1.0 using the packages
586 LEA 3.4.0⁸⁹.

587

588 ***Gradient forest modelling***

589 For all predictions in gradient forest models, resampling was necessary because not
590 all environmental raster layers had the same resolution and extent. They were all cropped to
591 the latest-updated modelled and expert-validated species distribution¹² and reprojected to the
592 WorldClim bioclimatic rasters, as they have the highest resolution, using bilinear
593 interpolation or nearest neighbour method for continuous and categorical variables
594 respectively.

595 To correct for the genetic structure, spatial variables were generated using the
596 principal coordinates of neighbour matrices (PCNM) approach⁹⁰. Only half of the positive
597 PCNM values were kept. Gradient forest model was used to predict and rank the importance
598 of environmental variables in genomic variation, as its machine learning algorithm worked
599 best with minimal prior and confounding variables. Putatively neutral SNPs and putatively
600 adaptive SNPs were used as the response variables and all the filtered environment variables
601 and PCNM variables were used as the predictor variables in the gradient forest model for 500
602 regression trees. The maximum number of splits to evaluate was determined as follows:

$$\text{Maximum number of splits} = \log_2 \frac{(0.368 \times \text{number of predictor variables})}{2}$$

603

604 The turnovers of allelic frequencies were then projected spatially across the latest-
605 updated predicted species distribution ranges¹² using the fitted gradient forest model and the
606 environmental values across the range. Principal component analysis (PCA) was used to
607 summarise the genomic variation across the distribution and the first three principal
608 components (PC1, PC2, and PC3) were used for visualisation of genomic variation across the
609 range.

610 The PCAs of turnovers of allelic frequencies between adaptive SNPs and neutral
611 SNPs were compared using the Procrustes rotation, and its residuals were used to map where
612 adaptive genomic variation deviates from neutral variation.

613

614 ***Prediction of genomic vulnerability***

615 Future climate projections were obtained from five general circulation models (GCM)
616 (MIROC6, BCC-CSM2-MR, IPSL-CM6A-LR, CNRM-ESM2-1, MRI-ESM2-0)
617 participating in the World Climate Research Programme Coupled Model Intercomparison
618 Project 6 (WCRP CMIP6) for four shared socio-economic pathways (SSPs) (126, 245, 370,
619 and 585) over four 20-year periods (2021–2040, 2041–2060, 2061–2080, 2081–2100). The
620 gradient forest model was used to predict patterns of genetic variation and local adaptation
621 under future environmental scenarios. The allelic frequency turnover function was fitted on
622 the future landscape and the genomic offset, defined as the required genomic change in a set
623 of putatively adaptive loci to adapt to a future environment⁹¹, was calculated in a grid-by-grid
624 basis using the following equation for Euclidean distance, where p is the number of
625 environmental (predictor) variables:

$$\text{Genetic offset} = \sqrt{\sum_{n=1}^p (\text{Future allelic turnover} - \text{Current allelic turnover})^2}$$

626

627 The genetic offset was then scaled across all SSPs and time periods.

628

629 ***Prediction of genomic similarity between current germplasm source and future restoration***

630 ***site***

631 It is of practical interest to a range of forestry stake-holders to predict if a current
632 germplasm source is a good match for future restoration sites, or where to source suitable
633 germplasm for a proposed restoration site. We developed an interactive web application
634 based on R Shiny and hosted the application on the shinyapps.io server. *seeder* v 1.0 is open
635 source and freely available from <https://trainingidn.shinyapps.io/seeder/>. The analysis
636 workflow consists of the selection of species of interest, time period and future climate
637 scenario, and the restoration site's geographical coordinates (Supplementary Figure 11).

638 The application maps the predicted turnover of allelic frequencies at a hypothetical
639 future restoration site onto the current landscape on a grid-by-grid basis, with the genetic
640 offset calculated as described above. After scaling, the values are reversed on a 0-1 scale to
641 represent the genomic similarity between the current germplasm source and future restoration
642 site.

643

644 ***Data availability***

645 The research materials supporting this publication, including genomic assemblies, raw
646 reads, and annotations, can be publicly accessed either in the Supplementary Information or
647 in NCBI GenBank under the BioProjects PRJNA841235 and PRJNA841689.

648 **References**

- 649 1. UNODC. *World Wildlife Crime Report: Trafficking in Protected Species*. (2020).
650 2. UNODC. *World Wildlife Crime Report: Trafficking in Protected Species*. (United Nations
651 Publication, 2016).
652 3. United Nations Environment Programme. *The rise of environmental crime: A growing threat
653 to natural resources peace, development and security*. (2016).
654 4. Gaisberger, H. *et al.* Tropical and subtropical Asia's valued tree species under threat.
655 *Conservation Biology* **36**, e13873 (2022).
656 5. Winfield, K., Scott, M. & Graysn, C. Global status of *Dalbergia* and *Pterocarpus* rosewood
657 producing species in trade. in *Convention on International Trade in Endangered Species 17th
658 Conference of Parties - Johannesburg* (2016).
659 6. Asian Regional Workshop (Conservation & Sustainable Management of Trees Viet Nam).
660 *Dalbergia cochinchinensis*. The IUCN Red List of Threatened Species. e.T32625A9719096
661 (1998) doi:10.2305/IUCN.UK.1998.RLTS.T32625A9719096.en.
662 7. Nghia, N. H. *Dalbergia oliveri*. The IUCN Red List of Threatened Species 1998.
663 e.T32306A9693932 (1998) doi:10.2305/IUCN.UK.1998.RLTS.T32306A9693932.en.
664 8. CITES. *Consideration of proposals for amendment of appendices I and II. Convention on
665 International Trade in Endangered Species of Wild Fauna and Flora*. (Convention on
666 International Trade in Endangered Species of Wild Fauna and Flora, 2017).
667 9. Barstow, M. *et al.* *Dalbergia cochinchinensis*. *The IUCN Red List of Threatened Species 2022*
668 (2022).
669 10. Barstow, M. *et al.* *Dalbergia oliveri*. *The IUCN Red List of Threatened Species 2022* (2022).
670 11. Gaisberger, H. *et al.* Range-wide priority setting for the conservation and restoration of Asian
671 rosewood species accounting for multiple threats and ecogeographic diversity. *Biol Conserv*
672 **270**, 109560 (2022).
673 12. Myers, N., Mittermeier, R. A., Mittermeier, C. G., da Fonseca, G. A. B. & Kent, J.
674 Biodiversity hotspots for conservation priorities. *Nature* **403**, 853–858 (2000).
675 13. Woodruff, D. S. Biogeography and conservation in Southeast Asia: how 2.7 million years of
676 repeated environmental fluctuations affect today's patterns and the future of the remaining
677 refugial-phase biodiversity. *Biodivers Conserv* **19**, 919–941 (2010).
678 14. Wurster, C. M. *et al.* Forest contraction in north equatorial Southeast Asia during the Last
679 Glacial Period. *Proc Natl Acad Sci U S A* **107**, 15508–15511 (2010).
680 15. Jansen, M. *et al.* Food for thought: The underutilized potential of tropical tree-sourced foods
681 for 21st century sustainable food systems. *People and Nature* **2**, 1006–1020 (2020).
682 16. Oldekop, J. A. *et al.* Forest-linked livelihoods in a globalized world. *Nature Plants* **2020** 6:12
683 **6**, 1400–1407 (2020).
684 17. Centre for Forest, Landscape and Planning, D., Cambodia Tree Seed Project & Forestry
685 Administration, C. Conservation of valuable and endangered tree species in Cambodia 2001-
686 2006 - a case study. *Forest & Landscape: Development and Environment Series* **3**, (2006).
687 18. Version, D. *Conservation of valuable and endangered tree species in Cambodia 2001 - 2006*
688 *Moestrup, Søren; Sloth, Arvid; Burgess, Sarah*. (2017).
689 19. Maningo, E. v. & Thea, S. *Regional project for prootion of forest rehabilitation in Cambodia
690 and Vietnam through demonstration models and improvement of seed supply system: lesson
691 learned*.
692 20. APFORGEN. *Conserving Rosewood genetic resources for resilient livelihoods in the Mekong
693 - Project Inception Workshop Report*. (2018).
694 21. Frankham, R. *et al.* Loss of genetic diversity reduces ability to adapt. in *Genetic Management
695 of Fragmented Animal and Plant Populations* (eds. Frankham, R. *et al.*) (Oxford University
696 Press, 2017). doi:10.1093/OSO/9780198783398.003.0004.
697 22. Savolainen, O., Lascoux, M. & Merilä, J. Ecological genomics of local adaptation. *Nat Rev
698 Genet* **14**, 807–820 (2013).
699 23. Verkerk, P. J. *et al.* Climate-Smart Forestry: the missing link. *For Policy Econ* **115**, 102164
700 (2020).

- 701 24. Petit-Cailleux, C. *et al.* Tree Mortality Risks Under Climate Change in Europe: Assessment of
702 Silviculture Practices and Genetic Conservation Networks. *Front Ecol Evol* **9**, 582 (2021).
- 703 25. Lindner, M. *et al.* Climate change and European forests: What do we know, what are the
704 uncertainties, and what are the implications for forest management? *J Environ Manage* **146**,
705 69–83 (2014).
- 706 26. Hung, T. H. *et al.* Reference transcriptomes and comparative analyses of six species in the
707 threatened rosewood genus *Dalbergia*. *Sci Rep* **10**, 17749 (2020).
- 708 27. Supple, M. A. & Shapiro, B. Conservation of biodiversity in the genomics era. *Genome Biol*
709 **19**, (2018).
- 710 28. Allendorf, F. W., Hohenlohe, P. A. & Luikart, G. Genomics and the future of conservation
711 genetics. *Nat Rev Genet* **11**, 697–709 (2010).
- 712 29. Desalle, R. & Amato, G. Conservation Genetics, Precision Conservation, and De-extinction.
713 *Hastings Center Report* **47**, S18–S23 (2017).
- 714 30. Luo, X., Chen, S. & Zhang, Y. PlantRep: a database of plant repetitive elements. *Plant Cell*
715 *Rep* **41**, 1163–1166 (2022).
- 716 31. Hartvig, I. *et al.* Population genetic structure of the endemic rosewoods *Dalbergia*
717 *cochinchinensis* and *D. oliveri* at a regional scale reflects the Indochinese landscape and life-
718 history traits. *Ecol Evol* **8**, 530–545 (2018).
- 719 32. Hartvig, I. *et al.* Conservation genetics of the critically endangered Siamese rosewood
720 (*Dalbergia cochinchinensis*): recommendations for management and sustainable use.
721 *Conservation Genetics* 1–16 (2020) doi:10.1007/s10592-020-01279-1.
- 722 33. Roy, D. & Sadanandom, A. SUMO mediated regulation of transcription factors as a
723 mechanism for transducing environmental cues into cellular signaling in plants. *Cellular and*
724 *Molecular Life Sciences* **78**, 2641–2664 (2021).
- 725 34. Lee, J. *et al.* Salicylic acid-mediated innate immunity in Arabidopsis is regulated by SIZ1
726 SUMO E3 ligase. *The Plant Journal* **49**, 79–90 (2007).
- 727 35. Catala, R. *et al.* The Arabidopsis E3 SUMO ligase SIZ1 regulates plant growth and drought
728 responses. *Plant Cell* **19**, 2952–2966 (2007).
- 729 36. Yoo, C. Y. *et al.* SIZ1 Small Ubiquitin-Like Modifier E3 Ligase Facilitates Basal
730 Thermotolerance in Arabidopsis Independent of Salicylic Acid. *Plant Physiol* **142**, 1548–1558
731 (2006).
- 732 37. Jin, J. B. *et al.* The SUMO E3 ligase, AtSIZ1, regulates flowering by controlling a salicylic
733 acid-mediated floral promotion pathway and through affects on FLC chromatin structure.
734 *Plant J* **53**, 530–540 (2008).
- 735 38. Bay, R. A. *et al.* Predicting Responses to Contemporary Environmental Change Using
736 Evolutionary Response Architectures. *Am Nat* **189**, 463–473 (2017).
- 737 39. Hung, T. H. *et al.* Physiological responses of rosewoods *Dalbergia cochinchinensis* and *D.*
738 *oliveri* under drought and heat stresses. *Ecol Evol* (2020) doi:10.1002/ece3.6744.
- 739 40. Aerts, R. *et al.* Site requirements of the endangered rosewood *Dalbergiaoliveri* in a tropical
740 deciduous forest in northern Thailand. *For Ecol Manage* **259**, 117–123 (2009).
- 741 41. Nix, H. A. A biogeographic analysis of Australian elapid snakes. in *Atlas of elapid snakes of*
742 *Australia: Canberra, Australian Flora and Fauna Series 7* (ed. Longmore, R.) 4–15
743 (Australian Government Publishing Service, 1986).
- 744 42. Moles, A. T. *et al.* Global patterns in plant height. *Journal of Ecology* **97**, 923–932 (2009).
- 745 43. Woodcock, D. & Shier, A. Wood specific gravity and its radial variations: the many ways to
746 make a tree. *Trees 2002 16:6* **16**, 437–443 (2002).
- 747 44. Garnier-Géré, P. H. & Ades, P. K. Environmental Surrogates for Predicting and Conserving
748 Adaptive Genetic Variability in Tree Species. *Conservation Biology* **15**, 1632–1644 (2001).
- 749 45. Aitken, S. N., Yeaman, S., Holliday, J. A., Wang, T. & Curtis-McLane, S. Adaptation,
750 migration or extirpation: climate change outcomes for tree populations. *Evol Appl* **1**, 95–111
751 (2008).
- 752 46. Supple, M. A. *et al.* Landscape genomic prediction for restoration of a Eucalyptus foundation
753 species under climate change. *Elife* **7**, e31835 (2018).
- 754 47. Manel, S. *et al.* Broad-scale adaptive genetic variation in alpine plants is driven by temperature
755 and precipitation. *Mol Ecol* **21**, 3729–3738 (2012).

- 756 48. Ledoux, J. B. *et al.* Potential for adaptive evolution at species range margins: contrasting
757 interactions between red coral populations and their environment in a changing ocean. *Ecol*
758 *Evol* **5**, 1178 (2015).
- 759 49. Gougherty, A. V., Keller, S. R. & Fitzpatrick, M. C. Maladaptation, migration and extirpation
760 fuel climate change risk in a forest tree species. *Nature Climate Change* **2021 11:2** **11**, 166–
761 171 (2021).
- 762 50. Jalonen, R., Valette, M., Boshier, D., Duminil, J. & Thomas, E. Forest and landscape
763 restoration severely constrained by a lack of attention to the quantity and quality of tree seed:
764 Insights from a global survey. *Conserv Lett* **11**, e12424 (2018).
- 765 51. Fremout, T. *et al.* Diversity for Restoration (D4R): Guiding the selection of tree species and
766 seed sources for climate-resilient restoration of tropical forest landscapes. *Journal of Applied*
767 *Ecology* **59**, 664–679 (2022).
- 768 52. Aitken, S. N. & Whitlock, M. C. Assisted Gene Flow to Facilitate Local Adaptation to Climate
769 Change. *Annu Rev Ecol Evol Syst* **44**, 367–388 (2013).
- 770 53. Bozzano, M. *et al.* *Genetic Considerations in Ecosystem Restoration Using Native Tree*
771 *Species*. (FAO and Bioversity International, 2014).
- 772 54. Breed, M. F., Stead, M. G., Ottewell, K. M., Gardner, M. G. & Lowe, A. J. Which provenance
773 and where? Seed sourcing strategies for revegetation in a changing environment. *Conservation*
774 *Genetics* **14**, 1–10 (2013).
- 775 55. Martins, K. *et al.* Landscape genomics provides evidence of climate-associated genetic
776 variation in Mexican populations of *Quercus rugosa*. *Evol Appl* **11**, 1842–1858 (2018).
- 777 56. Shafer, A. B. A. *et al.* Genomics and the challenging translation into conservation practice.
778 *Trends Ecol Evol* **30**, 78–87 (2015).
- 779 57. R. Taylor, H., Dussex, N. & van Heezik, Y. Bridging the conservation genetics gap by
780 identifying barriers to implementation for conservation practitioners. *Glob Ecol Conserv* **10**,
781 231–242 (2017).
- 782 58. Shafer, A. B. A. *et al.* Genomics and the challenging translation into conservation practice.
783 *Trends Ecol Evol* **30**, 78–87 (2015).
- 784 59. Belaghzal, H., Dekker, J. & Gibcus, J. H. Hi-C 2.0: An optimized Hi-C procedure for high-
785 resolution genome-wide mapping of chromosome conformation. *Methods* **123**, 56 (2017).
- 786 60. Matthey-Doret, C. *et al.* *koszullab/hicstuff: Use miniconda layer for docker and improved P(s)*
787 *normalisation*. (2020) doi:10.5281/ZENODO.4066363.
- 788 61. Baudry, L. *et al.* InstaGRAAL: Chromosome-level quality scaffolding of genomes using a
789 proximity ligation-based scaffolder. *Genome Biol* **21**, 1–22 (2020).
- 790 62. Cabanettes, F. & Klopp, C. D-GENIES: dot plot large genomes in an interactive, efficient and
791 simple way. *PeerJ* **6**, e4958 (2018).
- 792 63. Flynn, J. M. *et al.* RepeatModeler2 for automated genomic discovery of transposable element
793 families. *Proc Natl Acad Sci U S A* **117**, 9451–9457 (2020).
- 794 64. Bao, Z. & Eddy, S. R. Automated De Novo Identification of Repeat Sequence Families in
795 Sequenced Genomes. *Genome Res* **12**, 1269 (2002).
- 796 65. Price, A. L., Jones, N. C. & Pevzner, P. A. De novo identification of repeat families in large
797 genomes. *Bioinformatics* **21 Suppl 1**, (2005).
- 798 66. Benson, G. Tandem repeats finder: a program to analyze DNA sequences. *Nucleic Acids Res*
799 **27**, 573–580 (1999).
- 800 67. Tarailo-Graovac, M. & Chen, N. Using RepeatMasker to Identify Repetitive Elements in
801 Genomic Sequences. *Curr Protoc Bioinformatics* **25**, 4.10.1-4.10.14 (2009).
- 802 68. Ellinghaus, D., Kurtz, S. & Willhoeft, U. LTRharvest, an efficient and flexible software for de
803 novo detection of LTR retrotransposons. *BMC Bioinformatics* **9**, 1–14 (2008).
- 804 69. Steinbiss, S., Willhoeft, U., Gremme, G. & Kurtz, S. Fine-grained annotation and classification
805 of de novo predicted LTR retrotransposons. *Nucleic Acids Res* **37**, 7002–7013 (2009).
- 806 70. Li, W. & Godzik, A. Cd-hit: a fast program for clustering and comparing large sets of protein
807 or nucleotide sequences. *Bioinformatics* **22**, 1658–1659 (2006).
- 808 71. Cheng, C.-Y. *et al.* Araport11: a complete reannotation of the *Arabidopsis thaliana* reference
809 genome. *The Plant Journal* **89**, 789–804 (2017).

- 810 72. Bertoli, D. J. *et al.* The genome sequences of *Arachis duranensis* and *Arachis ipaensis*, the
811 diploid ancestors of cultivated peanut. *Nat Genet* **48**, 438–446 (2016).
- 812 73. Holt, C. & Yandell, M. MAKER2: An annotation pipeline and genome-database management
813 tool for second-generation genome projects. *BMC Bioinformatics* **12**, 491 (2011).
- 814 74. Korf, I. Gene finding in novel genomes. *BMC Bioinformatics* **5**, 1–9 (2004).
- 815 75. Stanke, M., Diekhans, M., Baertsch, R. & Haussler, D. Using native and syntenically mapped
816 cDNA alignments to improve de novo gene finding. *Bioinformatics* **24**, 637–644 (2008).
- 817 76. Chan, P. P. & Lowe, T. M. tRNAscan-SE: Searching for tRNA genes in genomic sequences.
818 *Methods Mol Biol* **1962**, 1 (2019).
- 819 77. Manni, M., Berkeley, M. R., Seppey, M., Sim~ Ao, F. A. & Zdobnov, E. M. BUSCO Update:
820 Novel and Streamlined Workflows along with Broader and Deeper Phylogenetic Coverage for
821 Scoring of Eukaryotic, Prokaryotic, and Viral Genomes. *Mol Biol Evol* **38**, 4647–4654 (2021).
- 822 78. Inglis, P. W., Pappas, M. de C. R., Resende, L. V. & Grattapaglia, D. Fast and inexpensive
823 protocols for consistent extraction of high quality DNA and RNA from challenging plant and
824 fungal samples for high-throughput SNP genotyping and sequencing applications. *PLoS One*
825 **13**, e0206085 (2018).
- 826 79. Torkamaneh, D., Laroche, J. & Belzile, F. Fast-GBS v2.0: an analysis toolkit for genotyping-
827 by-sequencing data. <https://doi.org/10.1139/gen-2020-0077> **63**, 577–581 (2020).
- 828 80. Joshi, N. A. *sabre* - A barcode demultiplexing and trimming tool for FastQ files. Preprint at
829 (2013).
- 830 81. Martin, M. Cutadapt removes adapter sequences from high-throughput sequencing reads.
831 *EMBnet J* **17**, 10–12 (2011).
- 832 82. Li, H. Aligning sequence reads, clone sequences and assembly contigs with BWA-MEM.
833 *ArXiv* **1303.3997**, (2013).
- 834 83. Danecek, P. *et al.* Twelve years of SAMtools and BCFtools. *Gigascience* **10**, 1–4 (2021).
- 835 84. Rimmer, A. *et al.* Integrating mapping-, assembly- and haplotype-based approaches for calling
836 variants in clinical sequencing applications. *Nature Genetics* **46**, 912–918 (2014).
- 837 85. Danecek, P. *et al.* The variant call format and VCFtools. *Bioinformatics* **27**, 2156–2158
838 (2011).
- 839 86. Frichot, E., Mathieu, F., Trouillon, T., Bouchard, G. & François, O. Fast and efficient
840 estimation of individual ancestry coefficients. *Genetics* **196**, 973–983 (2014).
- 841 87. Martins, H., Caye, K., Luu, K., Blum, M. G. B. & François, O. Identifying outlier loci in
842 admixed and in continuous populations using ancestral population differentiation statistics.
843 *Mol Ecol* **25**, 5029–5042 (2016).
- 844 88. Yang, J. *et al.* Genomic inflation factors under polygenic inheritance. *European Journal of*
845 *Human Genetics* **19**, 807 (2011).
- 846 89. Frichot, E. & François, O. LEA: An R package for landscape and ecological association
847 studies. *Methods Ecol Evol* **6**, 925–929 (2015).
- 848 90. Borcard, D. & Legendre, P. All-scale spatial analysis of ecological data by means of principal
849 coordinates of neighbour matrices. *Ecol Modell* **153**, 51–68 (2002).
- 850 91. Rellstab, C., Dauphin, B. & Exposito-Alonso, M. Prospects and limitations of genomic offset
851 in conservation management. *Evol Appl* **14**, 1202–1212 (2021).
- 852
- 853

854 **Competing interests statement**

855 The authors declare no competing interests.

856

857 **Author contributions**

858 T.H.H.: designed the study, processed the samples, conducted the Oxford Nanopore
859 sequencing, conceived and conducted the bioinformatic analyses, drafted the manuscript, and
860 secured funding for the project;

861 T.S.: collected the samples, revised the manuscript, and secured funding for the project;

862 B.T.: collected the samples, revised the manuscript, and secured funding for the project;

863 V.C.: collected the samples, and revised the manuscript;

864 I.T.: collected the samples, revised the manuscript, and secured funding for the project;

865 C.P.: collected the samples, and revised the manuscript;

866 S.B.: collected the samples, and revised the manuscript;

867 I.H.: collected the samples, and revised the manuscript;

868 H.G.: provided expertise and materials for species distribution models, and revised the
869 manuscript;

870 R.J.: revised the manuscript, and secured funding for the project;

871 D.H.B.: supervised the study, revised the manuscript, and secured funding for the project;

872 J.J.M.: designed and supervised the study, revised the manuscript, and secured funding for
873 the project.

874

875 **Acknowledgements**

876 The genomic work was supported by funding to T.H.H. from the Biotechnology and
877 Biological Sciences Research Council (grant number BB/M011224/1) and to T.H.H., J.J.M.
878 from the Google Cloud Academic Grant. The sampling work was supported by funding to

879 T.S., B.T., I.T., R.J., D.H.B., J.J.M from the UK Darwin Initiative (ref. 25-023). The work of
880 H.G. and R.J. was supported by the CGIAR Fund Donors (<https://www.cgiar.org/funder>)
881 through the CGIAR Research Programme on Forests, Trees and Agroforestry. T.H.H. wishes
882 to thank Andrew Eckert and Stephen Harris as the examiners of his doctoral thesis, who
883 provided very constructive feedback that improved this paper.